BENTHAM OPEN

CrossMark

The Open Fuels & Energy Science Journal

RESEARCH ARTICLE

A Regenerative Braking Control Strategy for EVs Based on Real-Time Dynamic Loading of the Wheels

Ning Li[1,2,*], Xiaobin Ning[1] and Qiucheng Wang[1]

[1]*Zhejiang University of Technology, Hangzhou 310014, China*
[2]*Zhijiang College of Zhejiang University of Technology, Shaoxing 312030, China*

Abstract: This paper proposes a regenerative braking control strategy based on real-time dynamic loading (RTDL) of wheels. Based on the nonlinear relationship between a spring's resilience and displacement, this paper establishes 7-degrees of freedom (DOF) full vehicle model with nonlinear suspension. Then, a method based on suspension deformation is devised to calculate the wheels' dynamic load, and RTDL is used to calculate the braking force of the front and rear wheels. With the braking intensity and the battery state of charge (SOC) as input variables and the desired regenerative braking force as an output variable, we establish a regenerative braking control strategy based on RTDL and simulate it in ADVISOR software. Results show that the designed control strategy effectively improves the regenerative braking energy recovery efficiency by assuring braking stability, and verifies the rationality and feasibility of the proposed control strategy.

1. INTRODUCTION

Electric vehicle (EV) regenerative braking technology is key to saving energy and protecting the environment. By recovering the consumed energy of the EV in the frictional braking process and releasing it in the driving process, the amount of energy consumed can be decreased and the cruising range can be improved. To recover the vehicle braking energy from the driving wheel to the greatest extent possible along with braking stability whilst preventing wheels from locking, the braking forces of the front and rear axles must be reasonably distributed according to the control strategy [1 - 3].

Under the normal braking condition, the braking force distribution strategy is mainly divided into the ideal braking force distribution strategy, the maximum energy recovery strategy and the parallel braking force distribution strategy [4, 5]. The ideal braking force distribution strategy generally uses the fuzzy-control algorithm by considering the braking efficiency and SOC synthetically, as well as the distribution of the braking forces on the front and rear axles in the braking process. At present, research mainly focuses on the energy recovery efficiency and the braking distance using a simplified linear vehicle model to study the fuzzy-control rules between input and output variables [6 - 11]. The maximum energy recovery strategy maximises energy recovery through complex control. The present study focuses mainly on meeting braking regulations and achieving vehicle braking stability by studying some complex control strategies and optimisation methods in the simplified linear vehicle model, making the energy recovery efficiency of the vehicle as high as possible [12 - 14]. The parallel braking force distribution strategy maintains the original system unchanged, and connected a motor in parallel, by controlling the motor to recover the energy during braking. The present research deals with control strategies for regenerative braking using a linear simplified vehicle model and ensures that the regenerative braking force of the motor and the friction braking force of the original system can be well coordinated and effective at recovering the braking energy [15 - 18]. This research was conducted under ideal

* Address correspondence to this authors at the Zhijiang College of Zhejiang University of Technology, Shaoxing 312030, China; Tel: +86 15957154636; E-mail: wwwningning@126.com

conditions using a simplified vehicle model without considering the effects of nonlinear deformation of the suspension on energy recovery when braking, the braking force distribution or the design of control strategy based on the linear formula. In fact, when the vehicle is braking, the suspension produces nonlinear deformation, resulting in the transfer of the front and rear axle loads with the braking deceleration is nonlinear change, and the ideal braking force required by the front and rear wheels with braking deceleration being a nonlinear change, thus causing the early control strategy designed by a simplified vehicle model to become unapplicable.

In this paper, the influence of the suspension's nonlinear deformation on the energy recovery system is considered in terms of braking energy recovery. We build a vehicle model that considers the suspension's nonlinear deformation, and a control strategy is proposed for calculating the front and rear wheel's loads under deformation of the suspension, and in turn, the distribution of the braking force. We establish a regenerative braking control strategy based on RTDL and validate it using simulation with the ADVISOR software, inputting the braking intensity and battery SOC and obtaining the desired regenerative braking force as an output variable.

2. A NONLINEAR GEOMETRIC MODEL OF SUSPENSION FOR A 7-DOF VEHICLE

To study the influence of the front and rear wheels' braking force on the suspension's nonlinear deformation, this paper establishes a 7- DOF full vehicle model with nonlinear suspension, as shown in Fig. (**1**).
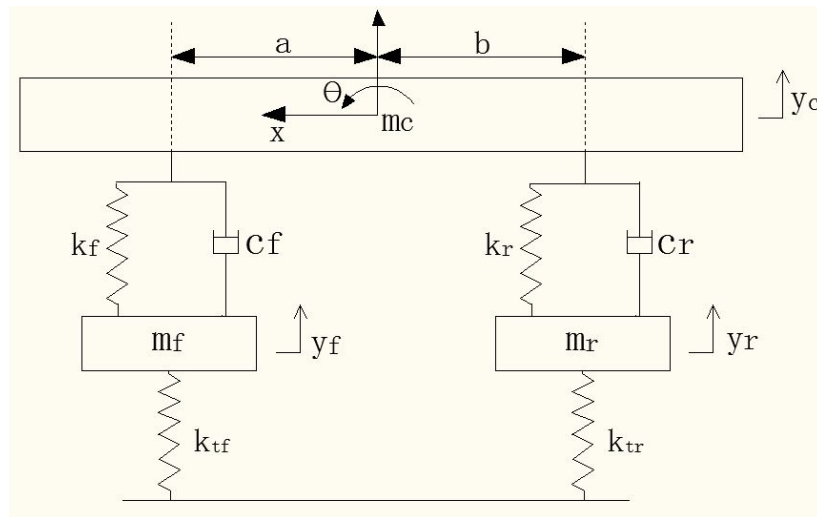

Fig. (1). A nonlinear geometric simplified model of the suspension of a 7-DOF vehicle.

According to refs [19, 20], the nonlinear spring-resilience-displacement is expressed as shown in Eqs. (1):

$$F = k_1(x_1 - x_2) + \varepsilon k_1(x_1 - x_2)^3 \tag{1}$$

where ε is the spring's nonlinear coefficient.

This paper establishes a suspension force equation while the vehicle is moving according to Eq. (1):

$$F_{sf} = k_f(y_c - a\sin\theta - y_f) + \varepsilon k_f(y_c - a\sin\theta - y_f)^3 + c_f(\dot{y}_c - a\sin\dot{\theta} - \dot{y}_f) \tag{2}$$

$$F_{sr} = k_r(y_c + b\sin\theta - y_r) + \varepsilon k_r(y_c + b\sin\theta - y_r)^3 + c_r(\dot{y}_c + b\sin\dot{\theta} - \dot{y}_r) \tag{3}$$

The sprung mass equations of motion are given by

$$m_c\ddot{y}_c + F_{sf} + F_{sr} = 0 \tag{4}$$

$$J_c\ddot{\theta} - m_c h_g\ddot{x} + F_{sr}b\cos\theta - F_{sf}a\cos\theta = 0 \tag{5}$$

The unsprung mass equations of motion are

$$m_r \ddot{y}_r + k_{tr} y_r - F_{sr} = 0 \tag{6}$$

$$m_f \ddot{y}_f + k_{tf} y_f - F_{sf} = 0 \tag{7}$$

The equations of motion for the wheels are

$$J_f \ddot{\omega}_f = F_{xf} R_f - T_f - T_{reb} \tag{8}$$

$$J_r \ddot{\omega}_r = F_{xr} R_r - T_r \tag{9}$$

And the wheel force's equations on the ground are given by

$$F_{zf} = m_c g b / L + m_f g - k_{tf} y_f \tag{10}$$

$$F_{zr} = m_c g a / L + m_r g - k_{tr} y_r \tag{11}$$

The vehicle's longitudinal kinetic equations are

$$m \frac{du}{dt} = F_{xf} + F_{xr} - F_f - F_w \tag{12}$$

$$F_f = mg(f_1 + f_2 u) \tag{13}$$

$$F_w = C_D A u^2 / 21.15 \tag{14}$$

Here, F_{sf} and F_{sr} are the forces on the front and rear suspensions, respectively, N; y_c is the displacement of the sprung mass, m; a is the distance from the centre of mass to the front axle, m; b is the distance from the centre of mass to the rear axle, m; L is the wheelbase, m; θ is the pitch angle of the vehicle when braking, deg; k_f and k_r are the spring stiffnesses of the front and rear suspensions, N/m; y_f and y_r are the unsprung mass displacements of the front and rear suspensions, m; c_f and c_r are the damping coefficients of the front and rear suspensions, $N/m/s$; m_c is the sprung mass, kg; J_c is the pitching moment of inertia of the sprung mass, $kg \cdot m^2$; x is the longitudinal displacement, m; h_g is the height of the vehicle's centre of mass, m; m_f and m_r are the unsprung masses of the front and rear suspensions, respectively, kg; J_f and J_r are the moments of inertia of the front and rear wheels, respectively, $kg \cdot m^2$; ω_f and ω_r are the angular velocities of the front and rear wheels, rad/s; R_f and R_r are the rolling radii of the front and rear wheels, rad/s; k_{tf} and k_{tr} are the vertical stiffness of the front and rear tyres, N/m; F_{zf} and F_{zr} are the normal applied forces of the front and rear wheels on the ground, respectively, N; m is the overall mass of the vehicle, kg; u is the vehicle speed, m/s; F_{xf} and F_{xr} are the braking forces on the front and rear wheels from the ground, N; F_y is the tire rolling resistance force, N; F_w is the air resistance, N; f_1 and f_2 are the rolling resistance coefficients; C_D is the air resistance coefficient; A is the vehicle's frontal area, m^2; T_f and T_r are the braking torques acting on the front and rear wheels of the braking system while braking, $N \cdot m$; and T_{reb} is the wheel torque supplied by the motor, $N \cdot m$.

3. THE PRINCIPLE OF BRAKING FORCE DISTRIBUTION BASED ON RTDL

3.1. Ideal Braking Force Distribution Principle

According to the ideal braking force distribution principle, on a road of any adhesion coefficient, the conditions that occur when the front and rear wheels lock simultaneously are given as follows: the sum of the braking forces on the front and rear wheels is equal to total adhesive force and they also respectively equal to themselves adhesive force [21], as shown in Eqs. (15 and 16):

$$F_{x1} = G \cdot \phi_f \cdot (b + z \cdot h_g) / L \tag{15}$$

$$F_{x2} = G \cdot \phi_r \cdot (a - z \cdot h_g) / L \tag{16}$$

Here, F_{x1} and F_{x2} are the front and rear wheels' braking forces, respectively, N; z is the braking intensity; $\varnothing_f$ and $\varnothing_r$

are the road adhesion coefficients of the front and rear wheels; G is the vehicle weight, N. For the linear vehicle model, as the deformation of the suspension is not considered, the ideal braking force needed by the front and rear wheels can be calculated from formulas 15 and 16.

For the nonlinear vehicle model affected by nonlinear deformation of the suspension, the load transfer between the front and rear axles and the braking deceleration is nonlinear when braking; thus, the front and rear braking forces cannot be distributed according to the linear formula of the ideal braking force distribution principle; in contrast, the front and rear wheel loads are needed to distribute braking force, as shown in Eqs. (17–19):

$$F_{xf} + F_{xr} = \varphi G \tag{17}$$

$$F_{xf} = \varphi F_{zf} \tag{18}$$

$$F_{xr} = \varphi F_{zr} \tag{19}$$

3.2. Principle of the Braking Force Distribution Based on RTDL

The front and rear wheel loads with brake deceleration variation change constantly under braking because the front and rear suspension stiffness are nonlinear; this makes accurately calculating the front and rear wheels' RTDL using a linear formula difficult. Therefore, the designed control strategy based on the linear vehicle model cannot guarantee the highest efficiency of energy recovery while also providing the best braking effect.

Therefore, this paper proposes a method to compute the RTDL of the front and rear wheels and to distribute the braking force according to the front and rear loading ratios by measuring the suspension deformation. While the vehicle is moving, the displacement (or deformation) y_f and y_r of the sprung masses of the front and rear suspensions, respectively, can be measured using a displacement sensor. We can then calculate the loads on the front and rear axles using Eqs. (10 and 11), and use their distribution ratio to distribute the front and rear wheels' braking forces, locking them simultaneously with the best brake effectiveness.

A vehicle usually has three running conditions-acceleration, constant velocity and braking, and the unsprung mass displacement also exists in three states-upwards motion, equilibrium position and downwards motion. In designing the control strategy, in order to recover regenerative energy only through braking, we use the measured unsprung mass displacements of the front and rear suspensions, y_f and y_r, respectively, where the unsprung mass equilibrium displacements of the front and rear suspensions are defined as zero when the vehicle is driving at a constant speed. This displacement is defined as negative as it moves downward with compression of the suspension and positive when it moves upward with the suspension's stretching. When the unsprung mass displacement of the front suspension is negative and that of the rear suspension is positive, we can distribute the braking forces of the front and rear wheels. In other cases, the unsprung mass displacements of the front and rear suspensions will be reset to zero, and no further steps are required. The schematic is shown in Fig. (**2**).
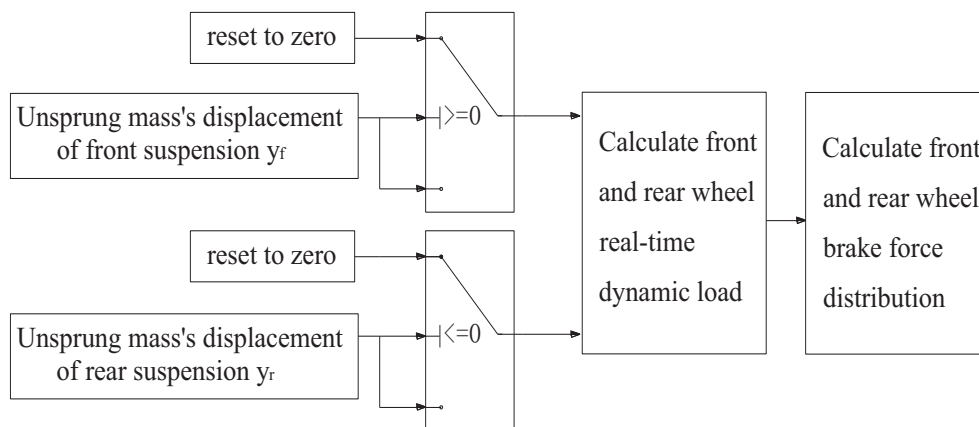
Fig. (2). Principle of calculating the braking forces of the front and rear wheels braking through unsprung mass displacement.

To recover as much energy as possible whilst ensuring the automobile brake stability, we define the total of braking

force to be taken on by the drive wheels when the braking intensity is relatively small ($z \leq 0.1$), and the rear wheel does not participate in vehicle braking. When the braking intensity is ($z > 0.1$), the braking force of the front and rear wheels will be distributed by RTDL, and the calculation process of the braking force distribution module based on RTDL is shown in Fig. (**3**).
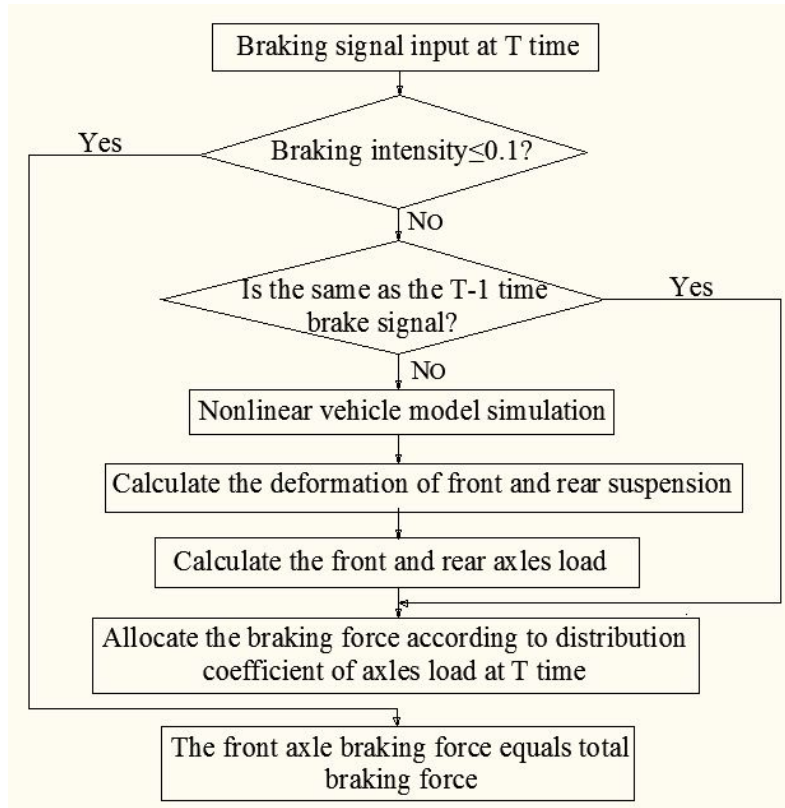

Fig. (3). The calculation process of the braking force distribution module based on RTDL.

4. FUZZY-CONTROL STRATEGY DESIGN FOR THE BRAKING FORCE BASED ON RTDL

4.1. The Principle of the Control Strategy Based on RTDL

With braking intensity z and the battery SOC as the fuzzy controller's input variables and the regenerative brake force coefficient K(regenerative braking force for front axle total braking force ratio) as the output variable, the fuzzy-control tactics schematic will be designed as shown in Fig. (**4**).
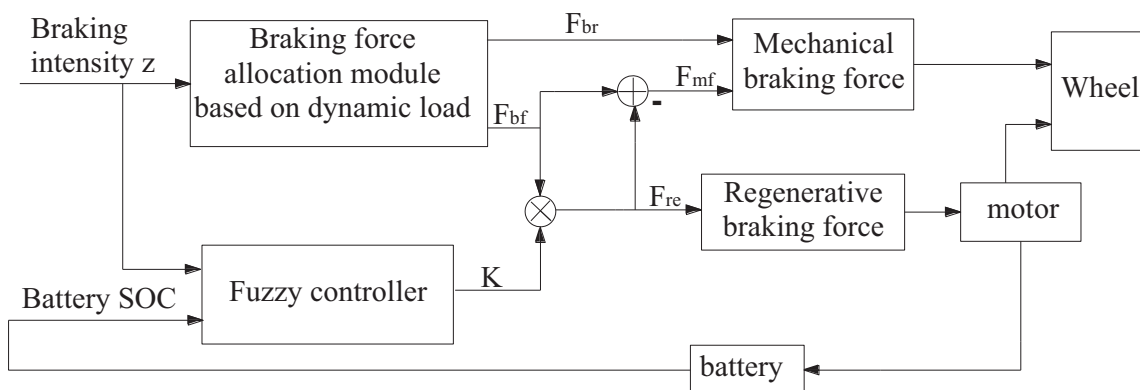

Fig. (4). Principle diagram of the fuzzy-control strategy for braking force based on RTDL.

When braking, the brake signal is transmitted to the brake force distribution module through the driver's input. This module can distribute the braking forces F_{bf} and F_{br} to the front and rear axles, respectively, according to the input of

the braking intensity signal. The braking force required by the rear wheel, F_{br} is the mechanical force, while that required by the front wheel, F_{bf} is the resultant force of the regenerative and mechanical braking forces. At the same time, fuzzy controller calculated the braking force coefficient K according to the input of the braking intensity z and the battery SOC, and with the front axle total braking force F_{bf} to do product operation; then, we obtain the front wheel's regeneration braking force F_{reb}. The front wheel's total braking force F_{bf} minus the regenerative braking force F_{reb} yields the front wheel's mechanical braking force F_{mf}. The mechanical braking forces F_{mf} and F_{br} are the current state of the front and rear wheels that is required to be applied to the friction braking force, F_{reb} is the current state of the front wheel that needs to be applied the regenerative braking force, and accordingly F_{reb} is what needs to be applied to control the motor for braking energy recovery; the recovered energy is stored in the form of electrical energy stored in batteries.

4.2. The Design of the Fuzzy Controller

While braking, the vehicle is significantly affected by road conditions, the driver's intention and the conditions of the motor and the battery, which will show uncertainty and be nonlinear; it is impossible to express these considerations with a formula. Thus, when we determine the distribution of the braking force, a fuzzy-control technology can be used. Expressing the influence of the different factors (such as braking intensity z and battery SOC) on regenerative braking is easy by means of a fuzzy-logic technique, which can also express control rules that are hard to quantify expediently.

In this paper, a Mamdani-type fuzzy controller is used to control the regenerative and machinery braking forces using the brake intensity z and the battery's SOC as input variables. The regenerative braking force coefficient K is an output variable. The structure of the controller is shown in Fig. (**5**).
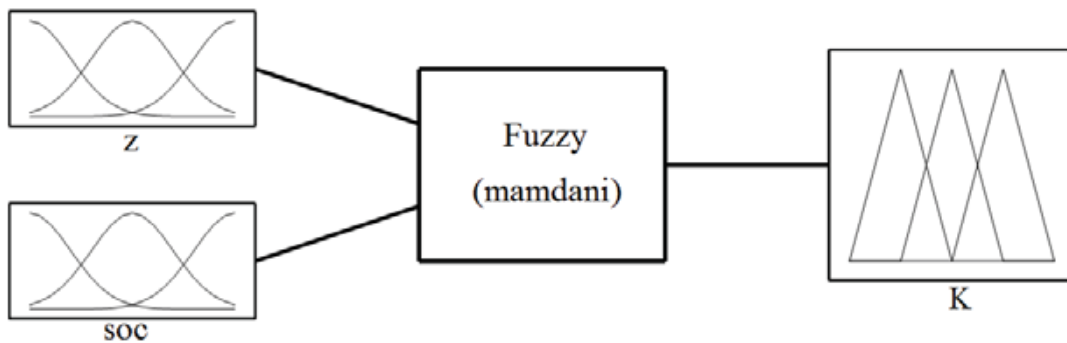

Fig. (5). Schematic diagram of the structure of a fuzzy controller.

The symbol z indicates the input variable braking intensity, which is subjected to a fuzzy transformation to allow it to be described in the fuzzy language. Finally, with fuzzy variables having values of middle-small (MS), small (S), middle (M), big (B) and middle-big (MB), the corresponding fuzzy subsets are set as {MS, S, M, B, MB}, the domain range is [0, 1] and the membership functions are as shown in Fig. (**6**).
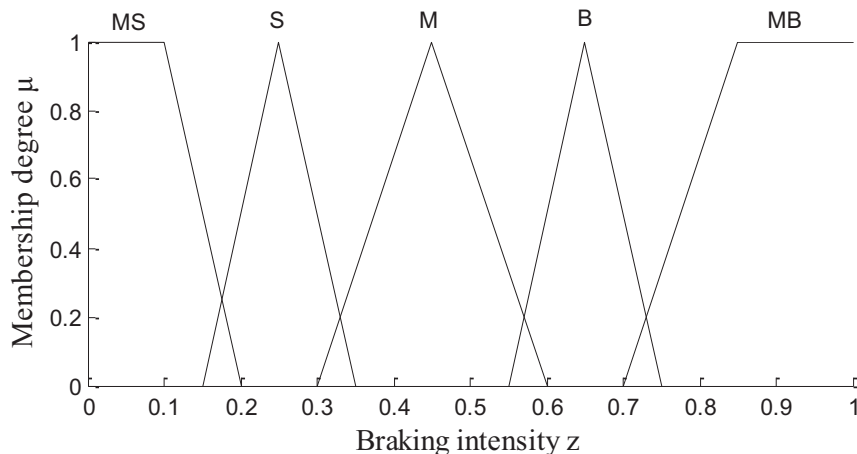

Fig. (6). The membership functions of braking intensity.

The symbol SOC indicates the input variable state of charge of the battery, which is subjected to a fuzzy transformation to allow it to be described in the fuzzy language. Finally, using fuzzy variables having values of very-small(VS), middle-small (MS), small (S), middle (M), big (B), middle-big (MB) and very-big (VB), the corresponding fuzzy subsets are set as {VS, MS, S, M, B, MB,VB}, the domain range is [0, 1] and the membership functions are as shown in Fig. (**7**).

The symbol K indicates the output variable regenerative braking force coefficient of front axle total braking force. which is subjected to a fuzzy transformation to allow it to be described in the fuzzy language. Finally, with fuzzy variables having values of very-small (VS), middle-small (MS), small (S), middle (M), big (B), middle-big (MB), very-big (VB), corresponding fuzzy subsets are set as {VS, MS, S, M, B, MB,VB}, the domain range is [0, 1] and the membership functions are as shown in Fig. (**8**).
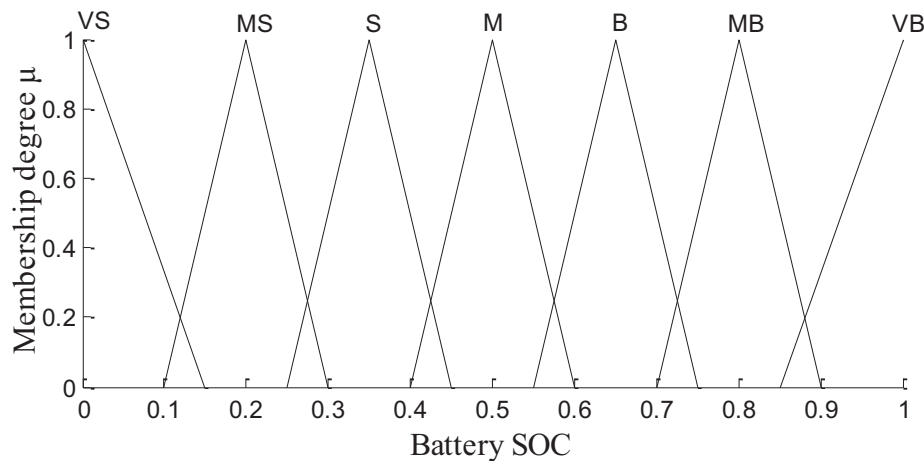

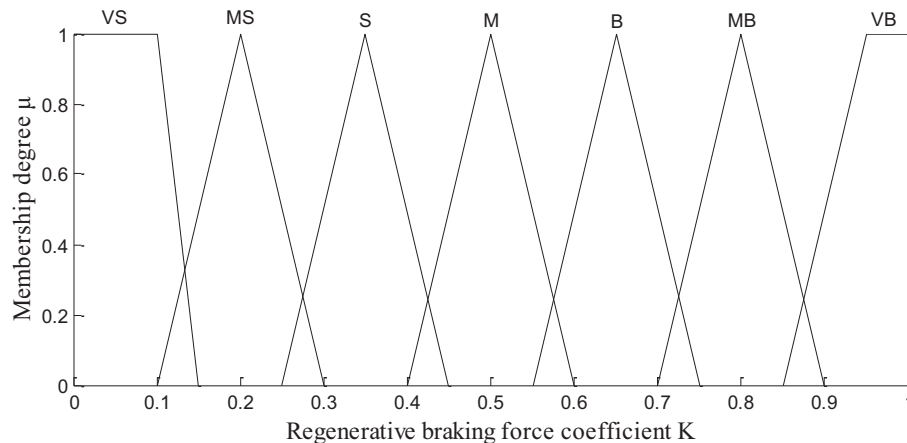**Fig. (7).** The membership functions of battery SOC.

**Fig. (8).** The membership functions of regenerative braking force coefficient K.

According to the braking intensity z, the battery SOC and the regenerative braking force coefficient K used to design fuzzy controller, the main design principles are as follows:

1. When the braking intensity is too high, to brake safely, minimum braking energy should be recovered; when the braking intensity is lower, maximum energy should be recovered.
2. When the SOC value is too high, the battery tends to be saturated. Thus, minimum braking energy should be recovered; when the SOC value is lower, maximum energy should be recovered.

Table **1** shows the final design of the fuzzy-rules. Fig. (**9**) shows the corresponding reasoning surface of the fuzzy controller.

Table 1. Fuzzy-rule table for the braking force distribution.

K		Z				
		MS	**S**	**M**	**B**	**MB**
SOC	VS	VB	VB	MB	MB	VS
	MS	VB	MB	MB	B	VS
	S	VB	MB	B	B	VS
	M	MB	MB	MB	B	VS
	B	MB	B	M	S	VS
	MB	B	M	S	MS	VS
	VB	M	S	MS	VS	VS
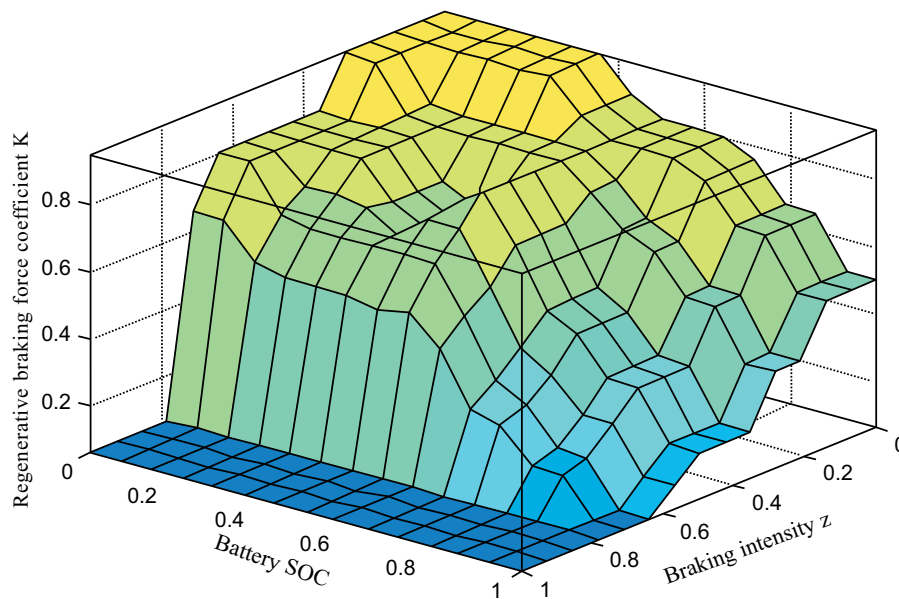
Fig. (9). Braking force distribution of the fuzzy controller's reasoning surface.

5. CONTRAST ANALYSIS BY SIMULATION WITH ADVISOR

A nonlinear vehicle model and braking force control strategy based on RTDL are constructed with SIMULINK software, and the model is embedded into ADVISOR software for simulation. The vehicle and main system parameters are shown in Table **2**. In the simulation model using ADVISOR, the front wheel uses a combination of regenerative and friction braking, whereas the rear wheel uses a pure friction brake. The energy of the front wheel is recovered during braking.

Table 2. Vehicle and main system parameters.

Vehicle	Mass	1617 kg
	Wheel base	2.75 m
	Height of the centre of mass	0.55 m
	Drag coefficient	0.35
	Tire radius	0.317
	Front suspension stiffness	32 N/mm
	Rear suspension stiffness	24 N/mm
Motor	Rated power	60 kw
	Maximum torque	210 Nm
	Maximum speed	8000 r/min
Power storage battery	Rated voltage	336 V
	Volume	60 A·h

The simulation is completed for two road conditions: the urban dynamometer driving schedule (CYC_UDDS), and

the road conditions of the city of Cleveland in the United States of America (CYC_CLEVELAND). The contrast between the two sets of road condition parameters is shown in Table **3**. CYC_UDDS are urban road conditions, the speed is low and the braking deceleration is small. CYC_CLEVELAND has high speeds and larger braking decelerations. The designs of the braking force control strategy based on RTDL and ADVISOR's own braking force control strategy are compared and simulated in ADVISOR. ADVISOR's own braking force control strategy was same as the mentioned control strategy of this paper in introduction part; it is based upon a linear vehicle model, and the influence of the suspension deformation upon the regenerative braking is not considered.

Under the CYC_UDDS and CYC_CLEVELAND conditions of the regenerative braking simulation, the battery SOC results under two conditions are shown in Figs. (**10** and **11**), respectively. Figs. (**12** and **13**) are the simulation results of unsprung mass displacement under two conditions; Table **4** compares the results of braking energy recovery under the two control strategies.

Table 3. The road condition parameters for CYC_UDDS and CYC_CLEVELAND.

	CYC-UDDS	CYC-CLEVELAND
Mileage (km)	11.99	16.43
Maximum speed (km/h)	91.25	161.43
Average speed (km/h)	31.51	93.14
Maximum acceleration (m/s^2)	1.48	3.09
Maximum deceleration (m/s^2)	-1.48	-7.98
Average acceleration (m/s^2)	0.5	0.84
Average deceleration (m/s^2)	-0.58	-1.64
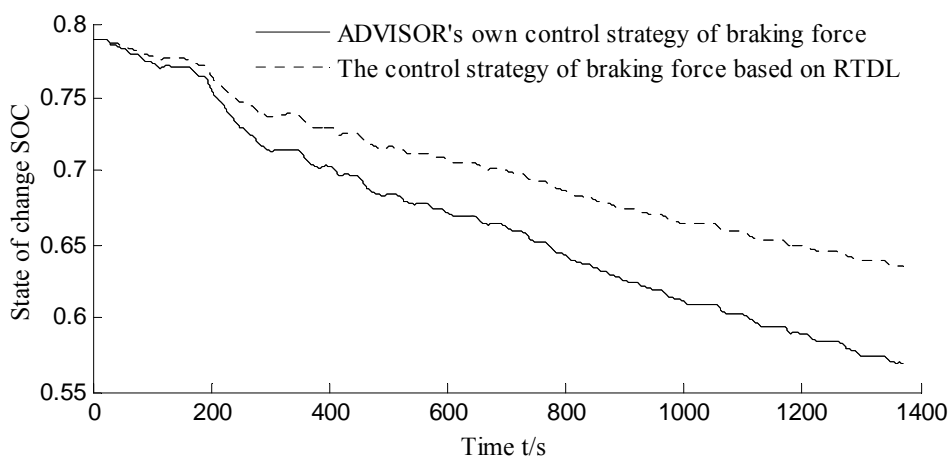
Fig. (10). The changing curve of the battery SOC under the circulation conditions of CYC_UDDS.
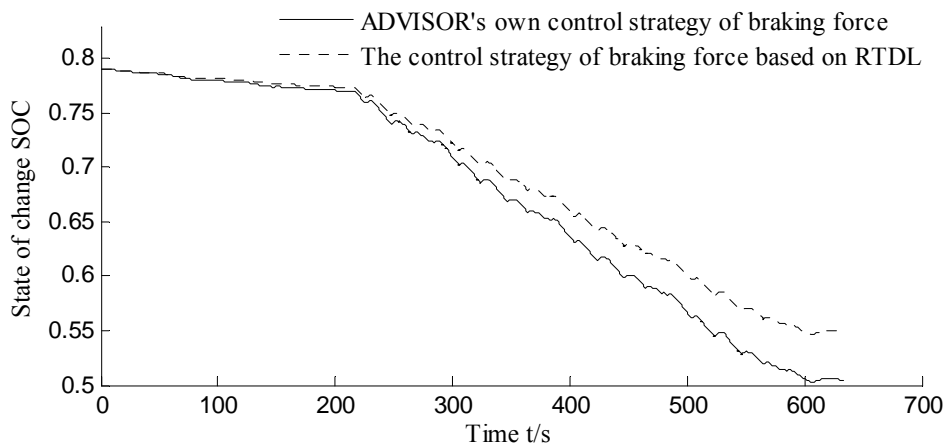
Fig. (11). The changing curve of the battery SOC under the circulation conditions of CYC_CLEVELAND.

As shown in Figs. (**10** and **11**), the braking force control strategy based on RTDL under both circulation conditions can slow the battery SOC while descending, especially under CYC_UDDS. The residual electricity in the storage battery has larger effects. The battery SOC value is 0.64, which is greater than ADVISOR's own braking force control strategy's value of 0.57 under the CYC_UDDS circulation condition, and it can also be seen that the battery recovered more braking energy.

The unsprung mass displacements of the front and rear suspensions during braking are shown in Figs. (**12** and **13**). We can see that those under CYC_CLEVELAND are larger than those under CYC_UDDS, and the braking intensity under the CYC_CLEVELAND circulation condition has a larger intensity. The CYC_CLEVELAND driving time is shorter than that under the CYC_UDDS condition, *i.e.* 634 s, compared with 1,369 s; thus, the simulation was completed faster for the CYC_CLEVELAND condition.
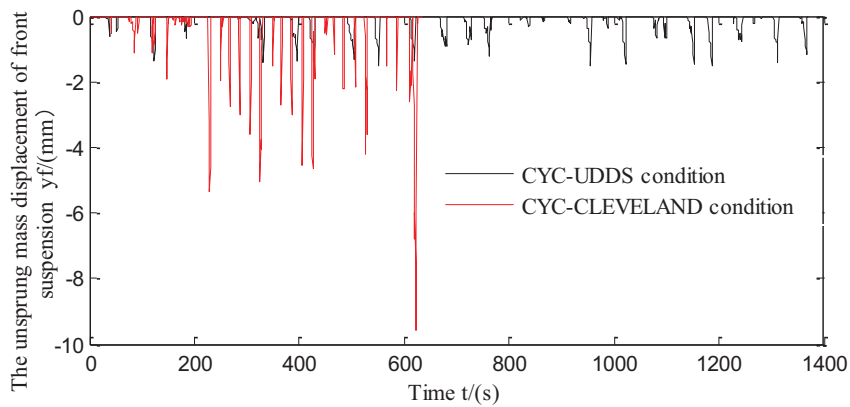

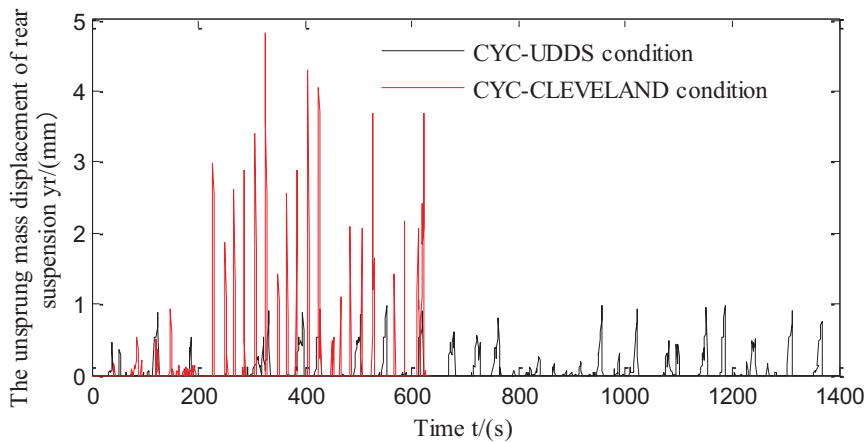**Fig. (12).** The unsprung mass displacement of the front suspension.

Fig. (13). The unsprung mass displacement of the rear suspension.

Table 4. Braking energy recovery under different control strategies.

	Target	ADVISOR's own control strategy	The braking force control strategy based on RTDL	Comparisons
CYC_UDDS	The total braking energy/KJ	2136	2136	Equal
	Regenerative braking energy/KJ	614	966	Improved by 57.33%
	Efficiency of regenerative braking energy recovery/%	28.74	45.22	Improved by 16.48%
CYC_CLEVELAND	The total braking energy/KJ	5669	5669	Equal
	Regenerative braking energy/KJ	2631	3175	Improved by 20.67%
	Efficiency of regenerative braking energy recovery/%	46.41	56.01	Improved by 9.6%

The brake energy regenerations under the different control strategies are shown in Table **4**. It can be seen that under

the CYC_UDDS condition, the control strategy proposed in this paper is superior to ADVISOR's own, the regenerative braking energy is increased by 57%, and the braking energy recovery inefficiency is increased by 16.48%. Under the CYC_CLEVELAND condition, the control strategy proposed in this study outperforms that of ADVISOR's own, the braking energy is increased by 20.67% and the recovery inefficiency of braking energy is increased by 9.6%.

The reason for this difference is the fact that CYC_UDDS represents city road circulation conditions; thus, the vehicle starts and brakes frequently, the average speed is 31.51 *km/h* and the greatest braking intensity is 0.15 (it is lower than 0.1 during most hours). According to the control strategy proposed in this paper, vehicle braking is often performed by the drive wheels (front wheels), with the rear wheels not participating in braking when the braking intensity is ≤0.1. Thus, the control strategy used in this paper can fully recover the braking energy in the circulation condition of CYC_UDDS. By contrast, ADVISOR's own control strategy for braking force is implemented using the methods of lookup tables, which distribute the front and rear wheels braking force based on the vehicle's speed, so that under a low braking intensity, there is a lower efficiency of braking energy recovery.

CYC_CLEVELAND offers high speed working conditions; the average speed is 93.14 *km/h* and the biggest braking intensity is 0.81. Under this circulation condition, the suspension deformation and load transfer are fairly large and represent nonlinear variations along with the brake deceleration. The front axle load calculated by the nonlinear vehicle model is bigger than those of the linear model, so the present front axle braking force is larger. Under the CYC _CLEVELAND conditions, the braking energy recovery efficiency of this paper's control strategy is higher than that of the ADVISOR's own control strategy due to the properties of linear and non-linear models.

Because the regenerative braking system and mechanical braking systems work together when the braking intensity is higher than 0.1 under the strategy proposed in this paper, the energy recovery efficiency under CYC _CLEVELAND is lower than that under CYC_UDDS.

CONCLUSION

1. According to the nonlinear relationship between a spring's resilience and its displacement, we established a 7-DOF full vehicle model with nonlinear suspension, considered the nonlinear deformation of suspension's influence upon regenerative braking and proposed a control strategy to distribute the braking force of front and rear wheels based on RTDL.
2. With the braking intensity and battery SOC as input variables and the regenerative braking force coefficient as an output variable, we designed a fuzzy controller, and subsequently, a fuzzy-control strategy for braking force based on RTDL is designed. We considered the suspension's deformation condition, braking intensity and battery power in the distribution of regenerative and machinery braking forces to the front and rear axles.
3. Using the ADVISOR software, the control strategy proposed in this paper based on RTDL was simulated and compared with ADVISOR's own strategy based on a linear vehicle model. The results showed that under the CYC_UDDS condition, the braking energy recovery efficiency of this paper's control strategy was higher than that of ADVISOR's own control strategy (16.48%); the same also held under the CYC_CLEVELAND condition, where the braking energy recovery efficiency of this paper's control strategy was higher than that of ADVISOR's own control strategy (9.6%).
4. Compared with the linear model control strategy used by ADVISOR, the control strategy proposed in this paper is closer to reality and has higher energy recovery efficiency; however, the strategy is complex and difficult to implement.

CONFLICT OF INTEREST

The authors confirm that this article content has no conflict of interest.

ACKNOWLEDGEMENTS

REFERENCES

[1]   Shi, Q.S. *Key Technologies Research on Energy Management Problems of Pure Electric Vehicles.* M.S. thesis, Shandong University: Shandong, **2009**.

[2]   Wang, M.; Sun, Z.C.; Zhuo, G.R. Braking energy recovery system for electric vehicle. *Trans. Chin. Soc. Agric. Mach.,* **2012**, *43*(2), 6-10.

[3]   Ning, X.B.; Li, N.; Jiang, J.P. Experiment of energy recovery efficiency and simulation research on EV's regenerative braking system. *Comput. Modell. New Technol.,* **2014**, *18*(9), 528-533.

[4]   Gao, Y.M.; Chen, L.P.; Ehsani, M. Investigation of the effectiveness of regenerative braking for EV and HEV. *SAE Paper 1999-01-2910,*

[5]   Glenn, B.; Washington, G.; Riszoni, G. Operation and control strategies for hybrid electric automobiles. *SAE Paper 2000-01-1537,* [http://dx.doi.org/10.4271/2000-01-1537]

[6]   Zhang, G.F.; Zhang, Z.J.; Xie, X.F.; Wang, G.X. Fuzzy logic in regenerative braking of EV. *J. Heilongjiang Inst. Sci. Technol.,* **2012**, *22*(2), 177-181.

[7]   Liu, H.; Wang, W.D.; He, J.; Xiang, C.L. Modeling and simulation of the regenerative braking system in a HEV based on fuzzy control. *Automot. Eng.,* **2012**, *34*(1), 51-56.

[8]   Wang, Y.N.; Liu, D.Q. A study of mechanical and electrical compound braking force distribution strategy for electric vehicle. *Kongzhi Gongcheng,* **2014**, *21*(3), 348-356.

[9]   Zhao, L.; Tang, L.; Wu, X.H. Distribution Strategy for electric vehicle braking force based on fuzzy control. *J. Desert Res.,* **2014**, *4*(41), 18-21.

[10]   Liu, L.J.; Ji, F.Z.; Yang, S.C.; Xu, B. Control strategy for electro-mechanical braking based on curves of ECE regulations and ideal braking force. *J. Beijing Univ. Aeronaut. Astronaut.,* **2013**, *39*(1), 138-142.

[11]   Gong, X.W.; Zhang, L.J.; Ma, J.; Wang, G.P. Braking force distribution of electric vehicles based on braking stability. *J. Chang'an Univ.,* **2014**, *34*(1), 103-108. [Natural Science Edition].

[12]   Guo, J.G.; Wang, J.P.; Cao, B.G. Brake force distribution strategy for electric vehicle based on maximum energy recovery. *J. Xi'an Jiaotong Univ.,* **2008**, *42*(5), 607-611.

[13]   Zhao, W.Z.; Gu, X.Y.; Wang, C.Y.; Hu, M.Y. Optimisation design of electro-hydraulic brake system with in-wheel electric vehicle. *J. Nanjing Univ. Aeronaut. Astronaut.,* **2013**, *45*(6), 871-874.

[14]   Yang, Y.J.; Zhao, H.Z.; Mao, F. A study on the control strategy for maximum energy recovery by regenerative braking in electric vehicles. *Automot. Eng.,* **2013**, *35*(2), 105-111.

[15]   Wang, X.Y.; Gu, J.C.; Li, Y.H. The simulation for optimisation of parallel regenerative braking control strategy. *Comput. Appl. Software,* **2010**, *27*(12), 184-186.

[16]   Ko, J.W.; Ko, S.Y.; Kim, I.S. Cooperative control for regenerative braking and friction braking to increase energy recovery without wheel lock. *Int. J. Automot. Technol.,* **2014**, *15*(2), 253-262. [http://dx.doi.org/10.1007/s12239-014-0026-6]

[17]   Zhang, J.M.; Liu, J.L. Parallel composite regenerative braking control strategy for electric buses. *Mach. Des. Manuf.,* **2014**, *9*(1), 11-18. [http://dx.doi.org/10.1016/j.ijmachtools.2014.02.005]

[18]   Wang, M.; Sun, Z.C.; Zhuo, G.R.; Cheng, P. Braking energy recovery system for electric vehicle. *J. Transac. Chin. Soc. Agric. Mach.,* **2012**, *43*(2), 6-10.

[19]   Sheng, Y.; Wu, G.Q. A chaos research on vehicle nonlinear suspension system. *Automot. Eng.,* **2008**, *30*(1), 57-60.

[20]   Gao, Y.; Fan, J.W.; Pan, S.H.; Li, S.; Kong, F. Fractional-order fuzzy control method for vehicle nonlinear active suspension. *Zhongguo Jixie Gongcheng,* **2015**, *26*(10), 1403-1408.

[21]   Yu, Z.S. *Automobile Theory,* 5th ed; China Machine Press: Beijing, **2009**.